Cell Reports
Article

The Impact of Aminoglycosides on the Dynamics of Translation Elongation

Albert Tsai,[1,3] Sotaro Uemura,[1,4] Magnus Johansson,[1,5] Elisabetta Viani Puglisi,[1] R. Andrew Marshall,[1,6] Colin Echeverría Aitken,[1,7] Jonas Korlach,[8] Måns Ehrenberg,[5] and Joseph D. Puglisi[1,2,*]
[1]Department of Structural Biology
[2]Stanford Magnetic Resonance Laboratory
Stanford University School of Medicine, Stanford, CA 94305-5126, USA
[3]Department of Applied Physics, Stanford University, Stanford, CA 94305-4090, USA
[4]Omics Science Center, RIKEN Yokohama Institute, 1-7-22 Suehiro-cho, Tsurumi-ku, Yokohama City, Kanagawa 230-0045, Japan
[5]Department of Cell and Molecular Biology, Biomedical Center, Uppsala University, Box 596, S-751 24 Uppsala, Sweden
[6]McKinsey & Company–Silicon Valley, 3705A Hansen Way, Palo Alto, CA 94304, USA
[7]Department of Biophysics and Biophysical Chemistry, Johns Hopkins University School of Medicine, Baltimore, MD 21205-2185, USA
[8]Pacific Biosciences, 1380 Willow Road, Menlo Park, CA 94025, USA
*Correspondence: puglisi@stanford.edu
http://dx.doi.org/10.1016/j.celrep.2013.01.027

SUMMARY

Inferring antibiotic mechanisms on translation through static structures has been challenging, as biological systems are highly dynamic. Dynamic single-molecule methods are also limited to few simultaneously measurable parameters. We have circumvented these limitations with a multifaceted approach to investigate three structurally distinct aminoglycosides that bind to the aminoacyl-transfer RNA site (A site) in the prokaryotic 30S ribosomal subunit: apramycin, paromomycin, and gentamicin. Using several single-molecule fluorescence measurements combined with structural and biochemical techniques, we observed distinct changes to translational dynamics for each aminoglycoside. While all three drugs effectively inhibit translation elongation, their actions are structurally and mechanistically distinct. Apramycin does not displace A1492 and A1493 at the decoding center, as demonstrated by a solution nuclear magnetic resonance structure, causing only limited miscoding; instead, it primarily blocks translocation. Paromomycin and gentamicin, which displace A1492 and A1493, cause significant miscoding, block intersubunit rotation, and inhibit translocation. Our results show the power of combined dynamics, structural, and biochemical approaches to elucidate the complex mechanisms underlying translation and its inhibition.

INTRODUCTION

The ribosome is the molecular machine that rapidly and accurately interprets the genetic code on the messenger RNA (mRNA) to synthesize proteins (Green and Noller, 1997). During elongation, the ribosome repeats the cycle of selecting a transfer RNA (tRNA) molecule matching the codon in the 30S A site, incorporating the amino acid from the selected A-site tRNA into the polypeptide on the P-site tRNA, translocating the A- and P-site tRNAs to the P and E sites, and stepping precisely three bases in the 3′ direction (Korostelev et al., 2008; Wintermeyer et al., 2004; Zaher and Green, 2009). To elongate with an optimal balance of speed and accuracy, the ribosome employs G protein elongation factors (elongation factor thermo unstable [EF-Tu] and elongation factor G [EF-G] in bacteria) to facilitate key steps during the process (Nilsson and Nissen, 2005). Using the energy from guanosine triphosphate (GTP) hydrolysis, EF-Tu enhances the rate and specificity of tRNA selection and EF-G catalyzes translocation.

The central role of translation makes the ribosome a rich target for clinically important small-molecule antibiotics. They employ diverse strategies to interfere with translation and fall into several distinct classes, including macrolides, tetracyclines, and aminoglycosides (Benveniste and Davies, 1973; Böttger, 2006; Davies et al., 1965; Perzynski et al., 1979; Woodcock et al., 1991). Biochemical and structural studies of these antibiotics have shed light on their mechanism and have, in turn, provided clues to the molecular workings of the ribosome and its ligands (Yonath, 2005). Here, we focus on the clinically important aminoglycosides as a representative group of translational inhibitors.

Aminoglycosides contain a central deoxystreptamine ring with amino-sugar modifications (4,5 and 4,6 disubstituted deoxystreptamine) and include neomycin, paromomycin, gentamicin, kanamycin, and the fused-ring compound, apramycin. Aminoglycosides disrupt the fidelity of tRNA selection and block translocation (Benveniste and Davies, 1973; Davies and Davis, 1968; Davies et al., 1965). Nuclear magnetic resonance (NMR) and X-ray crystal structures (Fourmy et al., 1998) as well as biochemical and molecular biological studies (Böttger et al., 2001; Powers and Noller, 1991) have revealed the structural basis for specific aminoglycoside binding to bacterial ribosomes. Aminoglycosides bind in the major groove of the 16S ribosomal RNA (rRNA) decoding site, forming specific contacts

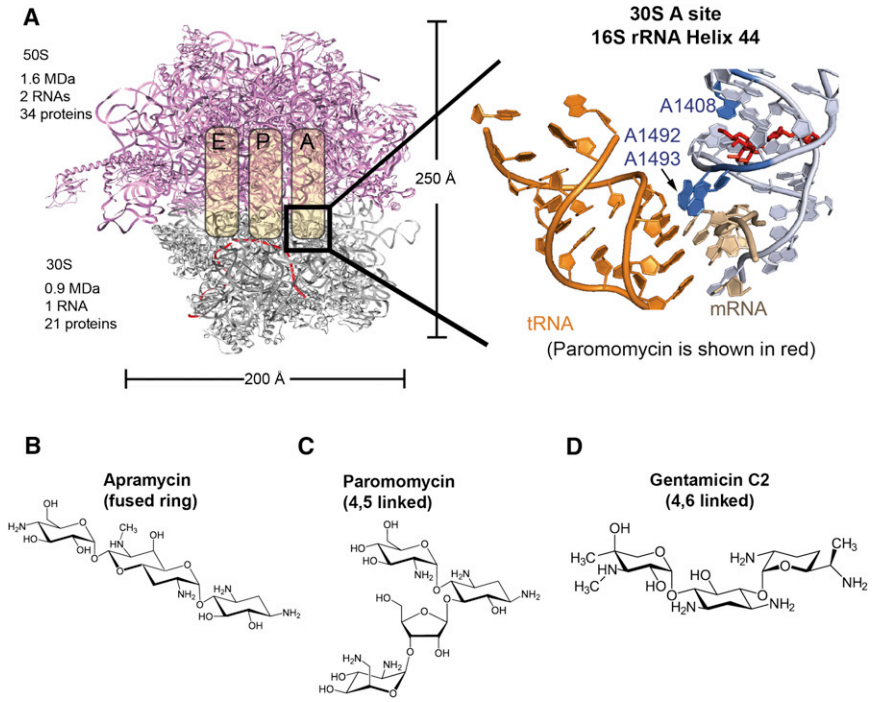

Figure 1. Aminoglycosides Bind in the 30S A Site in Helix 44 of the 16S rRNA

(A) The location where aminoglycosides bind to the bacterial ribosome is shown. The detailed binding site is shown to the right, with the A-site tRNA in orange and paromomycin in red. The three nucleotides in blue are A1408, which is specific to prokaryotes and conveys the specificity of aminoglycosides, and A1492/A1493, which are destacked by aminoglycosides and mimic the conformation of correct codon-anticodon recognition between the mRNA and the A-site tRNA. A-site structure with paromomycin is rendered from PDB 2J00 (Selmer et al., 2006).

(B–D) The structures of the three aminoglycosides tested. Biochemical experiments have shown that aminoglycosides induce miscoding and block translocation. Such effects were also seen in our single-molecule assays, as shown in Figure S1.

with conserved nucleotides G1494 and U1495; ring I of the aminoglycosides fits into a prokaryote-specific binding pocket formed by universally conserved nucleotides A1492 and A1493 and the prokaryotic-specific nucleotide A1408, imparting their specificity (Böttger et al., 2001; Recht et al., 1999).

These structural studies suggested a mechanism for aminoglycoside action (Figure 1A). In the presence of a cognate codon-anticodon complex, A1492 and A1493 (Moazed and Noller, 1990) make shape-specific contacts in the minor groove of the codon-anticodon A-form helix (Fourmy et al., 1998; Ogle et al., 2001; Yoshizawa et al., 1999). These contacts assist in distinguishing between correct and incorrect codon-anticodon pairings, as shown by both structural and kinetic investigations. In the absence of tRNA or drug, A1492/A1493 are stacked within an asymmetric internal loop at the base of Helix 44 (h44). Upon codon-anticodon interaction, A1492/A1493 are displaced from h44 to make the contacts discussed above. Binding of either 4,5 or 4,6 disubstituted aminoglycosides to the decoding site mimics this conformational effect, displacing A1492 and A1493 toward the minor groove.

Aminoglycosides alter the kinetics of tRNA accommodation, supporting these structural predictions (Pape et al., 1998, 2000). Paromomycin significantly reduces the dissociation rate of near-cognate tRNA and increases the rate of GTPase activation on EF-Tu by an order of magnitude. These results suggest that aminoglycosides stabilize near-cognate tRNA binding to the ribosome with a 16S rRNA conformation that mimics cognate codon-anticodon recognition. While the structural basis of aminoglycoside-induced miscoding has become clear, little is known about how they inhibit the subsequent steps of elongation. The relative importance of miscoding and inhibiting translocation to the potency of the drugs has not been determined. Here, we use a combined dynamics and structural approach to understand how distinct aminoglycosides disrupt translation.

We probed the mechanism of translational inhibition by an aminoglycoside from each of the three distinct structural classes: apramycin (fused-ring), paromomycin (4,5-linked), and gentamicin (4,6-linked) (Figures 1B–1D) using single-molecule, structural, and biochemical approaches. We solved the solution structure of apramycin bound to the bacterial decoding site by NMR spectroscopy, providing a structure to the repertoire of drug-RNA complexes. We determined the effects of all three drugs on the dynamics of translation using an array of single-molecule techniques (Aitken et al., 2010): we monitored the global conformation of the ribosome during elongation (Aitken and Puglisi, 2010) and the dynamics of tRNA accommodation by fluorescence resonance energy transfer (FRET) (Blanchard et al., 2004a) and used zero-mode waveguides (ZMW) to track multiple tRNAs through several elongation cycles at near physiological concentrations (Levene et al., 2003; Uemura et al., 2010). We also used bulk kinetics (Johansson et al., 2011) to measure the effects of aminoglycosides on rates of peptide bond formation and subsequent translocation. This combination of single-molecule dynamics, structural, and biochemical techniques reveals the mechanism of aminoglycoside action at an unparalleled level of detail.

RESULTS

Apramycin, Paromomycin, and Gentamicin Target Distinct Aspects of the Elongation Cycle

To monitor the global effects of aminoglycosides on elongation, we used intersubunit FRET between site-specifically labeled *Escherichia coli* 30S and 50S subunits (Aitken and Puglisi, 2010; Dorywalska et al., 2005; Marshall et al., 2008) that enable real-time monitoring of single ribosomes performing multiple elongation cycles. For each cycle of elongation, the ribosome rotates the 30S body relative to the 50S and then reverses the

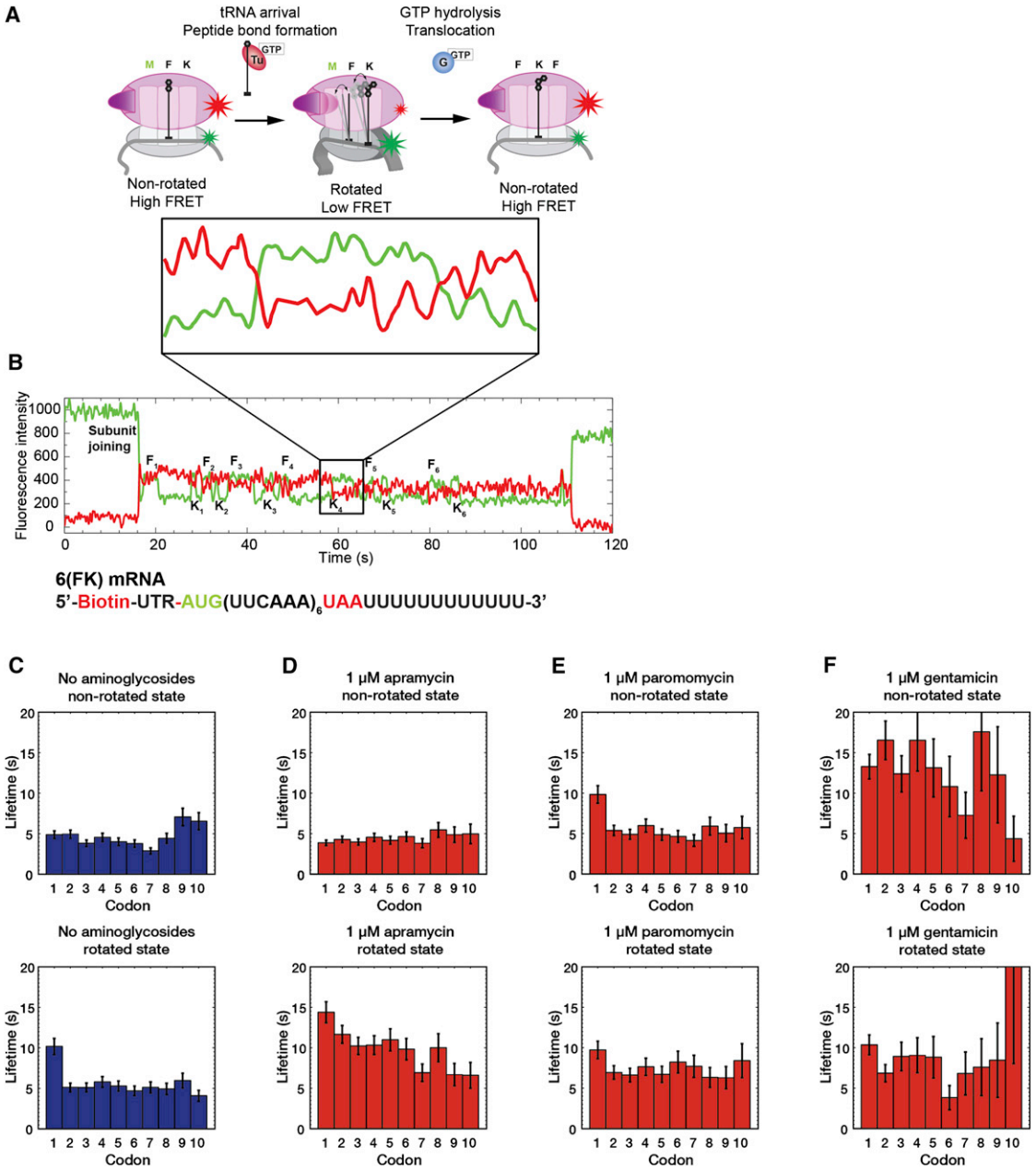

Figure 2. Aminoglycosides Inhibit Translation Elongation at Different Stages

(A) The intersubunit FRET signal involves cycles between a high FRET state where the 30S body of the ribosome is not rotated relative to the 50S subunit and a low FRET state, where the 30S body is rotated. From previous studies (Aitken and Puglisi, 2010; Marshall et al., 2008), peptide bond formation rotates the 30S body and causes a transition from high to low FRET. EF-G translocates and counterrotates the 30S body, causing a low to high FRET transition.

(B) An example trace of the intersubunit FRET, where the ribosome translated the entire 6(FK) mRNA. The zoomed panel directly below the diagram in (A) illustrates the changes in FRET state over one elongation cycle.

(C–F) The lifetimes that each ribosome spends in a conformation state over a given codon are fitted to a single exponential decay function and plotted. From left to right, the conditions are no aminoglycosides (C, n = 381), 1 μM apramycin (D, n = 429), 1 μM paromomycin (E, n = 264), and 1 μM gentamicin (F, n = 297). Error bars are SD errors. Different aminoglycosides target different aspects of translation elongation.

See also Figure S2 for lifetimes from additional experiments.

rotation, controlled respectively by peptide bond formation upon tRNA accommodation and translocation. The nonrotated state is detected by high FRET and the rotated state by a lower FRET value. The resultant FRET cycles report on the processivity and dynamics of the ribosome at each codon (Figures 2A and 2B) (Aitken and Puglisi, 2010). All three aminoglycosides significantly inhibited elongation efficiency (Figures S1A–S1C; see Extended Results for details). To probe the mechanistic origins

of translation inhibition by each aminoglycoside, we leveraged the ability of this single-molecule FRET approach to detect codon-specific effects on the dynamics of 30S body rotation and counterrotation during elongation (Figures 2C–2F and S2A–S2D) (Aitken and Puglisi, 2010; Marshall et al., 2008).

At 1 μM, apramycin did not measurably affect the lifetime (~4 s) of the high-FRET, or nonrotated state, where the ribosome selects tRNA and performs peptidyl transfer. In contrast, apramycin lengthened the low FRET, or rotated state, where the ribosome waits for EF-G to drive translocation by 2-fold from 5 s without drugs to ~10 s. Increasing apramycin concentration to 10 μM further increased the rotated ribosome lifetime to 3-fold (~15 s) longer than minus drugs, but did not otherwise introduce any additional effects on elongation. Increasing the EF-G concentration to 160 nM (from 80 nM, Figures S2E–S2G) partially rescued the rotated ribosome lifetime (1.6-fold longer than that minus drugs [~8 s]).

At 1 μM paromomycin, the nonrotated state lifetime of the ribosome at the first codon was increased 2-fold (~10 s), but was unaffected at subsequent codons. Paromomycin also lengthened the rotated state lifetime to a lesser extent by 1.4-fold (~7 s). Increasing the concentration to 10 μM further lengthened the first nonrotated state lifetime to 3-fold (~15 s) and the rotated state lifetimes to 2-fold of minus drugs (~10 s). Additionally, paromomycin lengthened the rotated state specifically over the first codon to 4-fold (~20 s) from normal. However, this effect is not observed at 1 μM, suggesting a possible alternative binding site (Borovinskaya et al., 2007). Overall, paromomycin displays a more complex set of effects on the elongation cycle and appears to participate in unique interactions with the ribosome at the first codon of the mRNA.

At 1 μM, gentamicin had the most severe effects on the nonrotated state lifetime, lengthening it by 3-fold (~15 s) across all codons, suggesting a mechanism distinct from paromomycin. However, similar to paromomycin, gentamicin slightly lengthened the rotated lifetime of the ribosome by 1.6-fold (~8 s). Addition of 10 μM gentamicin led to no further increase in the nonrotated ribosome lifetime; however, similar to paromomycin, a secondary effect of a lengthened rotated ribosome lifetime (to ~14 s, a 2.8-fold increase over no drugs) over the first codon was observed.

In addition to impacting different phases of elongation, the three aminoglycosides also induce different levels of miscoding, as described in the Extended Results (Figures S1D–S1F).

Following Real-Time tRNA Transit and Sampling in the Presence of Aminoglycosides Using ZMW

We next probed the dynamics of aminoglycoside action from the perspective of tRNA binding by directly tracking in real-time labeled tRNA binding and transit through the ribosome in zero mode waveguides (ZMW). The sequence, frequency, and length of each tRNA signal report on the fidelity of tRNA selection and on the speed of elongation was based on the dwell time of the tRNA (Figures 3A and 3B). We have used this approach previously to track ribosomal compositional dynamics during initiation and elongation (Tsai et al., 2012; Uemura et al., 2010).

In the absence of aminoglycosides, stable binding and transit of multiple tRNAs on the ribosome were observed as regular pulse cycles of repeating Cy5 followed by Cy2 signals with regular times between pulses of 10~20 s (Figures 3C, 3D, and S3A–S3C), as observed previously (Uemura et al., 2010). In the presence of 10 μM apramycin, the time between pulses lengthened significantly to 30~40 s, a nearly 2-fold increase, where the pulse sequence was still recognizable. Addition of 10 μM paromomycin and gentamicin introduces frequent metastable tRNA binding events of the length of 1 ~ 5 s, and the sequences of those events do not match the codon sequence of the 6(FK) mRNA used for the experiments (Figure 3E). The abundance of these short-lived events complicates the identification of binding events, resulting in accommodation and translocation. See the Extended Results for the detailed analysis on how the aminoglycosides alter tRNA binding behavior (Figures S3D–S3F). This result is consistent with our intersubunit FRET experiments that both aminoglycosides severely impact tRNA selection.

Following Real-Time tRNA Dynamics in the Presence of Aminoglycosides

To delineate the distinct effects of aminoglycosides on tRNA sampling and selection, we followed FRET between a P-site fMet-(Cy3)tRNA^{fMet} and an incoming A-site Phe-(Cy5)tRNA^{Phe} in the presence of antibiotics for an mRNA coding for Met-Phe-Lys (MFK). The evolution of this FRET signal reports on the decoding and accommodation of the A-site tRNA as well as classical to hybrid state fluctuations of the tRNA after peptide bond formation (Blanchard et al., 2004b; Figures 4 and S4A–S4C).

Apramycin did not significantly alter the dynamics of tRNA compared to no drugs. In both cases, FRET events proceeded to a high (0.8) FRET state within 100 ms of the appearance of FRET and subsequently fluctuated between high (0.8) and medium (0.5) FRET, consistent with rapid tRNA selection and accommodation and peptide bond formation followed by classical–hybrid dynamics (Blanchard et al., 2004b). However, apramycin increased the overall tRNA FRET lifetime from 10 s in the absence of drugs to 18 s (Table S1). By blocking of translocation, apramycin could prevent the eventual dissociation of tRNA^{fMet} from the E site, preserving FRET.

In contrast, paromomycin significantly altered the behavior of tRNA on the ribosome and induces many short-lived excursions (<1 s) from zero FRET to a high (>0.7) FRET level consistent with accommodated tRNA (Figure S4F). These events dropped the total FRET lifetime to 1.7 s. While these events are too long to be tRNA sampling attempts (<30 ms), they are much shorter than normal tRNA accommodation without drugs. Longer-lived (1~5 s) high-FRET events with little to no classical–hybrid state fluctuations were also observed (Figure S4G), consistent with single-molecule FRET measurements by Blanchard and coworkers (Feldman et al., 2010). Together with our ZMW measurements, these data suggest that paromomycin stabilizes tRNAs when they sample the A site and shifts the classical–hybrid tRNA conformation equilibrium strongly toward the classical state. The addition of EF-G enriched longer-lived events, as described in the Extended Results (Figure S4C).

Gentamicin induced behavior similar to that of paromomycin in tRNA-tRNA FRET experiments, with short (<1 s) high-FRET events suggesting that the A-site tRNA has proceeded nearly

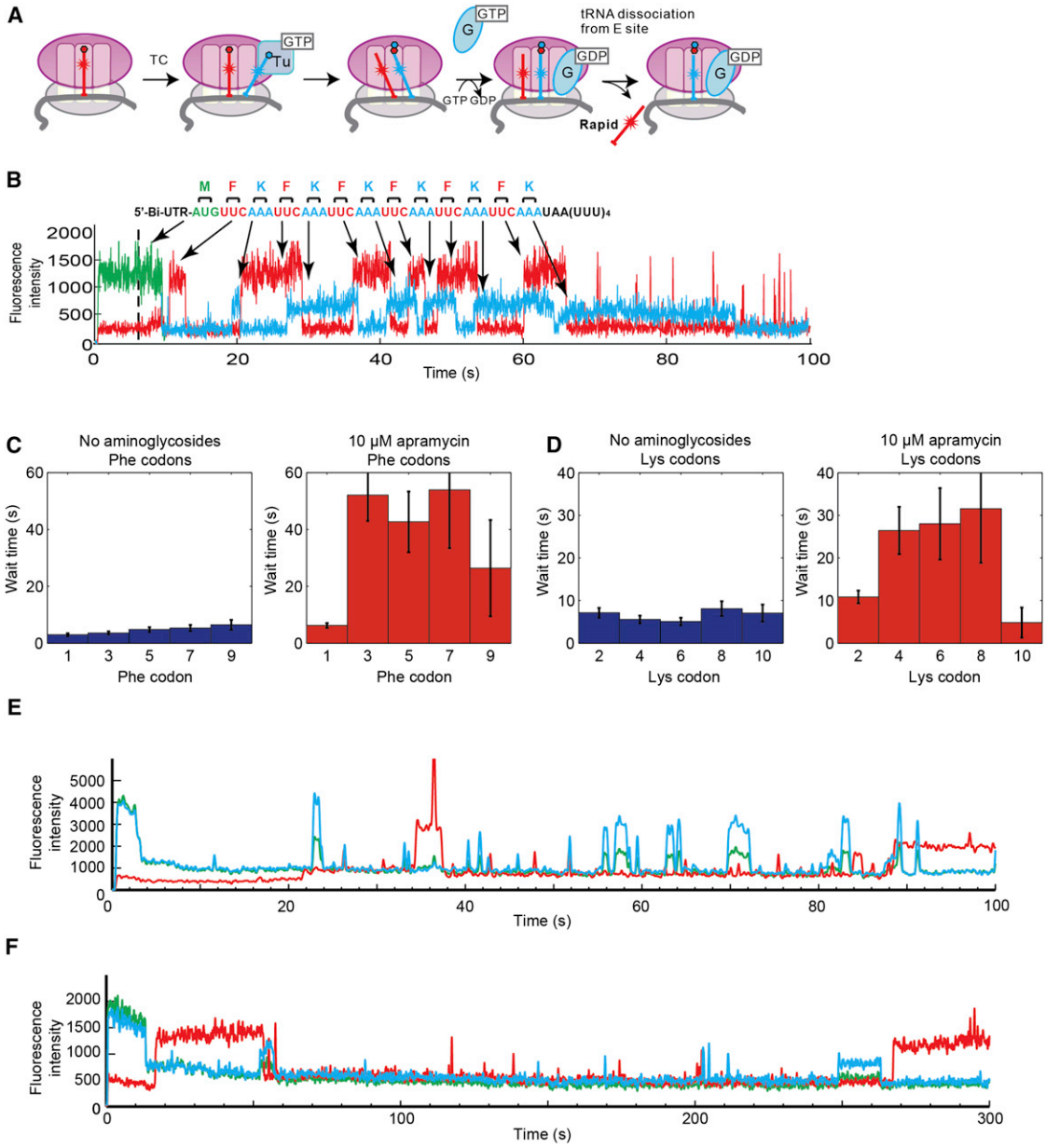

Figure 3. Aminoglycosides Alter tRNA Binding Patterns in ZMW tRNA Transit Experiments

(A) Using Phe-(Cy5)tRNA^{Phe} and Lys-(Cy2)tRNA^{Lys}, tRNA binding behavior and sequence can be observed and tRNA transit through the ribosome can be tracked. The tRNA signal lifetimes, wait times between tRNA events, and the frequency of the events can be tracked.

(B) An example trace of a tRNA transit experiment without aminoglycosides. The pulse sequence up to the last codon on the 6(FK) mRNA is well-behaved and can be analyzed codon-by-codon. Over the stop codon, short tRNA events are observed as tRNA sampling in the ribosomal A site. These types of events are greatly increased in the presence of paromomycin and gentamicin.

(C and D) The waiting times until the next tRNA event over each codon are plotted for the Phe (C) and Lys (D) codons. All error bars are SD. Paromomycin and gentamicin induce too many short tRNA events with the wrong sequence, which precludes an accurate analysis, as exemplified by the bottom two traces with 10 μM gentamicin.

(E) Many short tRNA binding events, whose sequence does not conform to the repeating Phe-Lys sequence encoded in the 6(FK) mRNA used in this experiment.

(F) A ribosome stalls after the first one or two codons and does not restart until nearing the end of the 300 s observation time in ZMW experiments.

See also Figure S3 for additional analysis of ZMW experiments.

to accommodation. A longer-lived high-FRET population with limited exchanges between the classical and hybrid tRNA conformations was also observed. These high-FRET events are longer lived than those observed in paromomycin, with a lifetime approaching the photobleaching time of the FRET pair (18 s). The overall fraction of the short-lived population is also

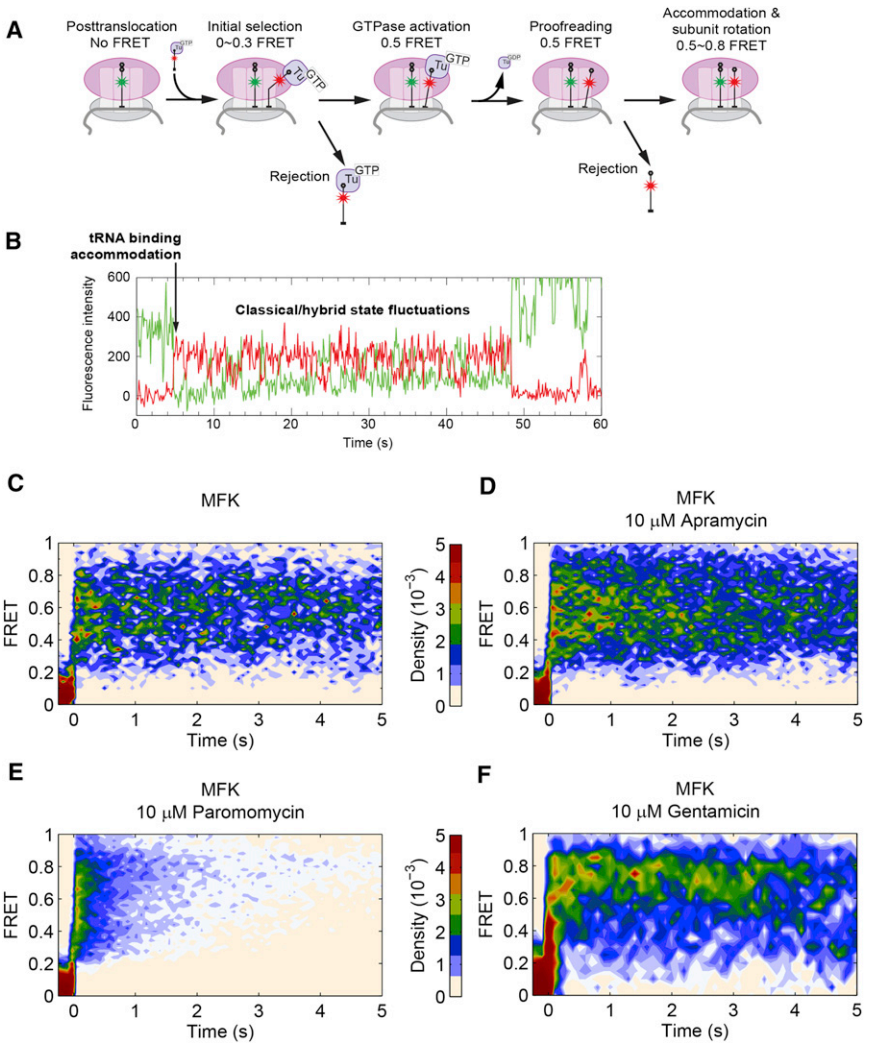

Figure 4. Paromomycin and Gentamicin Disrupts the Selection of the A-Site tRNA

(A) FRET between Cy3-labeled P-site tRNA and incoming Cy5-labeled A-site tRNA can be used to track tRNA selection. The evolution of this FRET signal reports on the dynamic decoding and accommodation of the A-site tRNA as well as classical to hybrid fluctuations of the tRNA upon peptide bond formation (Blanchard et al., 2004b).

(B) An example trace from a tRNA-tRNA FRET experiment without aminoglycosides on an MFK mRNA. The traces from tRNA-tRNA FRET experiments are then postsynchronized to have the first appearance of FRET to be $t = 0$. The condition for each panel is listed in the title.

(C) Without drugs on the MFK mRNA (n = 54), a high FRET (~0.75) signal appears and, within 100 ms, the tRNAs begin to fluctuate between the classical (~0.75 FRET) and hybrid (~0.5 FRET) conformations. The FRET signal is present for >10 s.

(D) Apramycin (n = 136) does not significantly affect the tRNA selection process.

(E) Paromomycin (n = 184) severely alters the behavior by introducing short (~1 s) high-FRET events and long events (>10 s) with limited classical/hybrid fluctuations.

(F) Gentamicin (n = 66) also introduces many sub 1 s events and long events with little classical/hybrid fluctuations.

See also Figure S4 for additional tRNA-tRNA FRET experiments and Table S1 for lifetimes of tRNA events.

lower than paromomycin, as shown in the higher relative density of the long events in the postsynchronized plot and the longer total tRNA lifetime (6.8 s). These differences suggest a mechanism distinct from paromomycin.

Paromomycin Induces Miscoding

To probe how paromomycin alters tRNA selection fidelity, we repeated our tRNA-tRNA FRET experiments with an mRNA encoding Met-Leu-Lys (MLK), in which the Leu codon is CUU, near-cognate to the Phe UUU codon. Delivery of Phe-(Cy5) $tRNA^{Phe}$ to immobilized ribosomes initiated with fMet-(Cy3) $tRNA^{fMet}$ in the P site tested the ability of the ribosome to distinguish between cognate and near-cognate tRNA in the A site. Without drugs and in the presence of apramycin, few detectable tRNA FRET events were observed. Thus, the ribosome was able to discriminate against the near-cognate tRNA; mRNA-independent binding events did not produce FRET and so were not detected in these experiments (Blanchard et al., 2004a).

In the presence of paromomycin, we observed many detectable tRNA FRET events on the near-cognate CUU codon (Figures S4D and S4E). Similar to the cognate mRNA experiment, we observed short excursions to high FRET as well as longer-lived (1~5 s) high-FRET events that showed very limited classical/hybrid fluctuations. The overall lifetime of tRNA FRET in these experiments (1.4~1.9 s) was unchanged as compared to tRNA FRET lifetimes on the cognate MFK mRNA with paromomycin. In contrast to the MFK cognate experiment, about 10% of longer-lived events (1~3 s) were locked in a medium-FRET state (~0.5), consistent with progression to EF-Tu GTPase activation but not full A-site accommodation (Lee et al., 2007). Pape and coworkers previously observed reduced rates of EF-Tu conformational change and tRNA accommodation after GTPase activation on a near-cognate codon by the addition of paromomycin (Pape et al., 2000). Overall, however, the behavior of tRNA on the cognate MFK and near-cognate MLK mRNAs was remarkably similar in the presence of paromomycin. These results further support the view that paromomycin interferes with the ribosome in distinguishing between cognate and near-cognate tRNA.

The Apramycin Binding Site on the Ribosome Is Distinct from that of Other Aminoglycosides

To explore the structural origins of apramycin function, we determined the NMR solution structure of apramycin in complex with

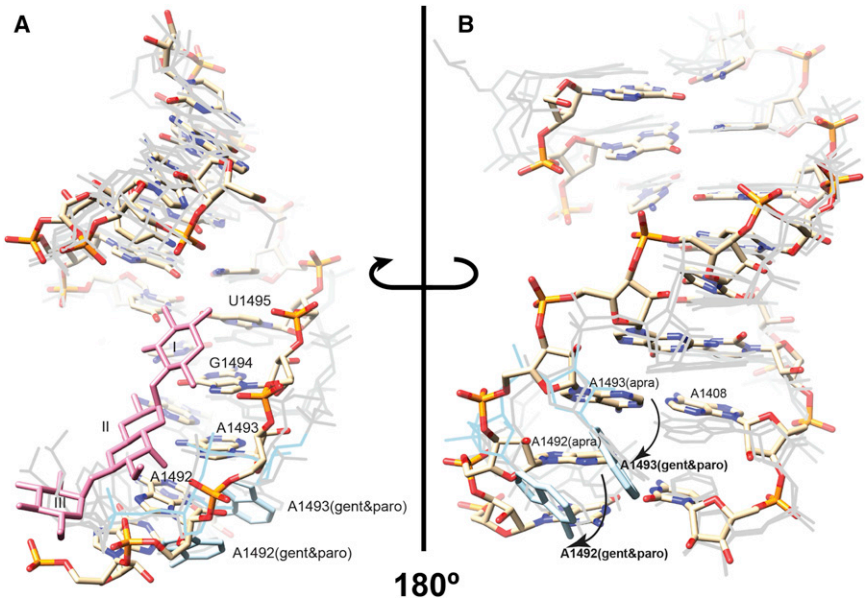

Figure 5. Apramycin Bound to the A Site Does Not Destack A1492/A1493

(A) The NMR solution structure with apramycin shown as lines and the 16S rRNA model shown as sticks (PDB ID 2M4Q). The three rings of apramycin (plum-colored) are labeled with roman numerals. The conformation of A1492 and A1493 with paromomycin and gentamicin bound is shown in light gray for comparison.

(B) The same NMR solution structure as (A) but viewed from the opposite site of helix 44. The apramycin-RNA complex structure is colored explicitly by atom. A1492 and A1493 (highlighted in light blue) with paromomycin and gentamicin are shifted with respect to their positions in the apramycin complex (indicated by the arrows). The overall structures of the paromomycin and gentamicin RNA structures are also shown in light gray for comparison, but apramycin is not shown for clarity.

See also Figure S5 and Table S2.

a 27-nucleotide RNA duplex that mimics the A site of the ribosome and the primary binding site of the aminoglycoside antibiotics (Recht et al., 1996). The NMR structure of paromomycin and gentamicin C with this model A-site oligonucleotide were previously published (Fourmy et al., 1996, 1998; Yoshizawa et al., 1998), and crystal structures with both oligonucleotide and ribosomal particles are available (Carter et al., 2000; François et al., 2005). Data on the RNA-apramycin complex were acquired on both unlabeled and uniformly ^{13}C, ^{15}N-labeled RNAs (Lukavsky et al., 2003; Lukavsky and Puglisi, 2005). A total of 623 nuclear Overhauser effect (NOE) distance restraints, including 32 drug-RNA NOEs, 111 dihedral restraints, and 23 residual dipolar coupling restraints were used in the structure calculations. The conformation of the drug-RNA interface was well defined by the NMR data: the root-mean-square deviation of the core RNA (U1406-U1410; A1490-U1495) and apramycin for the final 32 lowest energy structures was 1.21 Å (PDB ID 2M4Q).

As with all previous aminoglycoside-RNA complexes, including paromomycin and gentamicin C1a, apramycin binding to the A site was guided by interaction of the 2-deoxystreptamine ring with G1494 and U1495 (Figures 5 and S5) through hydrogen bonding interactions with N7 position of G1494 and the O4 position of U1495. However, the rigid structure of apramycin led to a distinct binding mode compared to that in the NMR structures of paromomycin- and gentamicin-RNA (Fourmy et al., 1996; Yoshizawa et al., 1998). Apramycin did not penetrate deeply in to the aminoglycoside binding pocket formed by A1408, A1492, and A1493, instead making stabilizing interactions with the phosphate backbone. As a result, apramycin did not stabilize the extrahelical, or destacked, conformation of A1492 and A1493 observed in the presence of paromomycin and other miscoding aminoglycosides. Apramycin binding to the oligonucleotide in solution favors the intrahelical, or stacked, conformation of the A1408, A1492, and A1493 observed in the structure of the free A-site oligonucleotide (Recht et al., 1996). Hygromycin B, another structurally unique, nonarchetypal antibiotic, binds the A site but does not cause destacking of A1492 and A1493; hygromycin B inhibits translocation without causing significant miscoding (Brodersen et al., 2000; Cabañas et al., 1978).

Effects of Apramycin, Paromomycin, and Gentamicin on Peptide Bond Formation Rates

The intersubunit FRET experiments show that paromomycin and gentamicin inhibit 30S body rotation during elongation. This could result from delays in peptide bond formation due to disruption in tRNA selection or steps subsequent to peptide bond formation. Accordingly, we assayed the effect of the three aminoglycosides on peptide bond formation kinetics in bulk experiments, as previously described (Johansson et al., 2011). The rates of GTP hydrolysis (k_{GTP}) and dipeptide formation (k_{pep}) for all three drugs remained unchanged compared to no drugs (Figure 6). As a control, we also measured the rate of formation of tripeptide (fMet-Phe-Phe) in each case (Figure S6). The rate of disappearance of f[^{3}H]Met, reflecting the rate of dipeptide formation, was also the same in each case. The rate of formation of tripeptides was, however, significantly decreased by the presence of each one of the drugs, in line with all three drugs slowing down the ribosome in elongation. These results suggest that the fraction of drug-bound ribosomes was close to 100% in the experiments.

DISCUSSION

Aminoglycosides are thought to affect translation by decreasing the fidelity of tRNA selection and blocking translocation. We employed a battery of complementary single-molecule methods, supported by structural and biochemical techniques, to form a coherent picture of the mechanism of action for three structurally distinct antibiotics: paromomycin, gentamicin C, and apramycin (Figure 7).

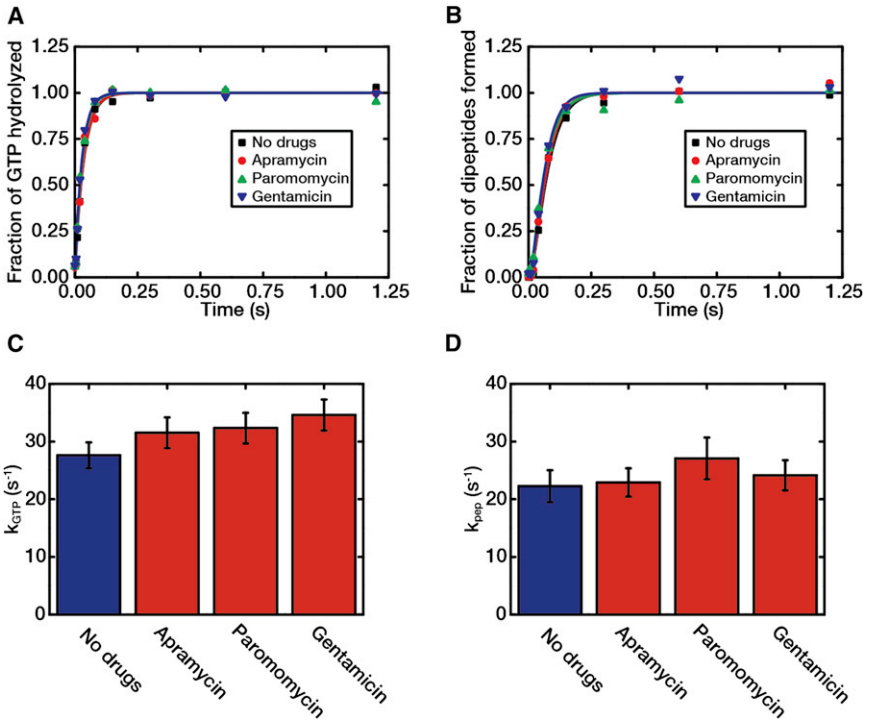

Figure 6. No Effect of Aminoglycosides on Peptide Bond Formation Rates

The extent of hydrolysis of EF-Tu-bound GTP (A) and dipeptide formation (B) were monitored over time upon mixing of Phe-tRNA^{Phe}:EF-Tu:GTP ternary complex with preinitiated 70S ribosomes in the presence or absence of each type of drug, as indicated in the figure. The rate of GTP hydrolysis, k_{GTP}, (C) and the rate of tRNA accommodation/peptidyl transfer, k_{pep}, (D) obtained from the inverse of the difference between the dipeptide formation time and GTP hydrolysis time were estimated for each case. Error bars in (C) and (D) represent SD as calculated from the fitting procedure averaged over two separate experiments (Johansson et al., 2011).

See also Figure S6.

Apramycin Slows Translation via One Primary Inhibition Mechanism

Apramycin has the clearest but the most atypical mode of action. The NMR solution structure of the apramycin-ribosomal RNA complex suggested a distinct structural mechanism for inhibition of translocation. The apramycin structure shows that the drug binds in the major groove of the 16S rRNA decoding site similar to other aminoglycosides. However, the drug does not induce the destacked conformation of A1492/A1493, as observed during correct codon-anticodon pairing. This differs with X-ray crystal structures showing A1492/A1493 destacked for all aminoglycosides (see Extended Discussion). However, the recent crystal structure of apramycin bound to the 30S subunit-tRNA-mRNA complex suggests that the drug would block unstacking of A1492 (Matt et al., 2012), consistent with this interpretation. The bias for a stacked conformation of A1492/A1493 in the presence of apramycin is supported by lower level of miscoding observed here and by others (Matt et al., 2012). This bias could additionally reduce the impact of apramycin on elongation dynamics over cognate codons prior to 30S body rotation, as evidenced by the normal nonrotated lifetime in intersubunit FRET, behavior in tRNA-tRNA FRET that is indistinguishable from no drugs, low tRNA sampling frequency in the ZMW (see Extended Discussion), and lack of effect on cognate k_{pep}.

Apramycin mainly blocks translocation; it significantly lengthens the rotated state lifetime, where the 70S complex is waiting for EF-G in order to translocate. While a previous single-molecule work (Feldman et al., 2010) has correlated inhibition in translocation to perturbations in tRNA conformational dynamics, apramycin breaks this trend, as it strongly inhibits translocation without inducing any noticeable increase in the occupancy of the classical tRNA conformational state in our tRNA-tRNA FRET experiment. Apramycin may instead lock the A site in an unfavorable conformation for EF-G, effectively increasing the energy barrier that EF-G must overcome to translocate. Similar effects have been observed for the translocation inhibitor spectinomycin, which binds the 30S subunit (Aitken and Puglisi, 2010). Apramycin inhibits the rate of elongation for about ten codons into the message, yet it gradually wears off such that the rotated-state lifetime has mostly recovered by the end of our 6(FK) mRNA. This suggests that the early phase of translation is more vulnerable to antibiotic action.

Paromomycin and Gentamicin Exhibit More Complex Modes of Action

Paromomycin disrupts multiple aspects of elongation, consistent with the conformational changes observed by structural methods. By favoring the destacked A1492/A1493 conformation (Fourmy et al., 1998), it causes severe miscoding in our stop codon readthrough assay. From tRNA-tRNA FRET experiments with a near-cognate codon (MLK) mRNA, the many observable events suggest that paromomycin slows the dissociation of an incorrect tRNA from the A site, consistent with prior kinetic measurements (Pape et al., 2000). Strikingly, paromomycin still retained half of its miscoding effect in our miscoding assay, where only the noncognate tRNA^{Phe} (to the stop codon) was present. As the total tRNA concentration in the experiment is halved, this result suggests tentatively that destacking of A1492/A1493 can induce miscoding with any tRNA available. The incorrect pulse sequence in ZMW experiments with paromomycin further demonstrates that the ribosome has lost its ability to distinguish correct codon-anticodon interactions.

The effects of paromomycin on elongation appear during both global conformational states of the ribosome and sometimes in a codon-specific manner. The frequent short tRNA FRET events indicate that the ribosome goes through many futile cycles where it accepts a tRNA into the A site, bypassing initial

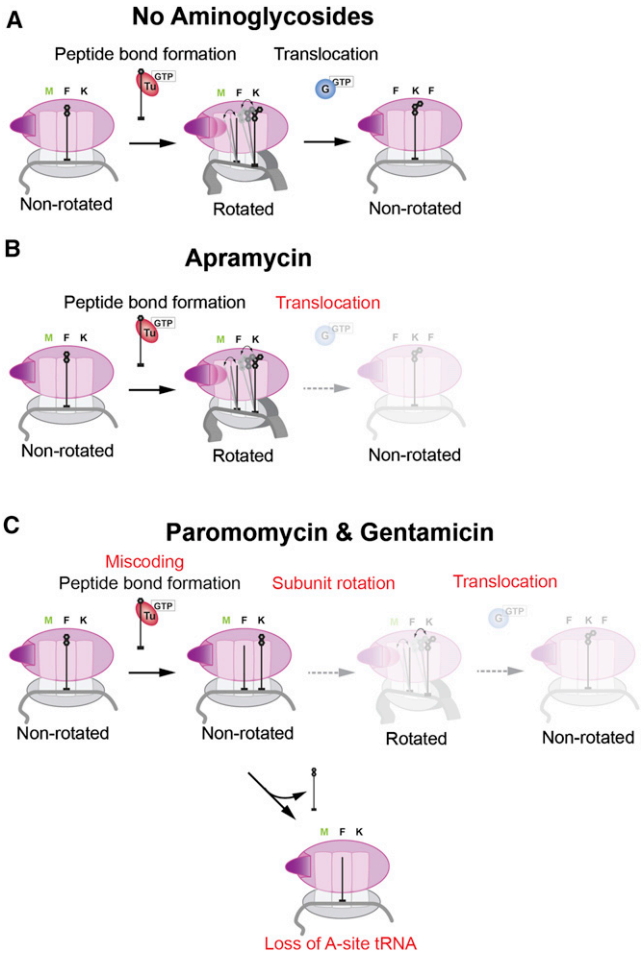

Figure 7. Aminoglycosides Disrupt Various Steps of Elongation

(A) In a normal elongation cycle, ribosome rotation occurs quickly after peptide bond formation between the A- and P-site tRNAs, allowing the tRNAs to fluctuate between the classical and hybrid states. EF-G then translocates and counterrotates the ribosome, moving the tRNAs into the P and E sites to reset the ribosome for another round of elongation.

(B) Apramycin does not hinder the rotation of the ribosome upon peptide bond formation; however, it blocks the translocation step where EF-G is involved. This mode of action differs from other members of the aminoglycoside family.

(C) Paromomycin and gentamicin display a more complex set of effects on elongation, slowing down both the rotation of the ribosome and translocation as well as inducing severe miscoding. With the ribosome stalled, the A-site tRNA could eventually dissociate with the short peptide chain due to a finite off-rate for tRNAs on the ribosome, leading to a stalled ribosome.

selection, but eventually rejects it. The high tRNA FRET level suggests that the A-site tRNA has proceeded beyond GTP hydrolysis by EF-Tu. Normal bulk peptide bond formation rate suggests that some tRNAs proceed as far as transferring the peptide chain from the P-site tRNA to the A-site tRNA. Combined with the increased nonrotated state lifetime in intersubunit FRET experiments, this suggests that paromomycin significantly increases the energy barrier to 30S body rotation, decoupling it from peptide bond formation. If a ribosome stalls early in elongation with a short peptide chain, it could risk losing the A-site tRNA by dissociation. Such ribosomes are left with a deacylated P-site tRNA and are unable to translocate normally, even when a correct tRNA binds in the A site, as indicated by the frequent short-lived binding events observed in the ZMW for stalled traces. Eventually, the ribosome might translocate spontaneously with an acylated A-site tRNA bound and reset itself with an amino acid on the P-site tRNA; however, accumulation of prematurely released peptidyl-tRNA could be toxic. Consistent with that hypothesis, some traces that halted at the first codon in both intersubunit FRET and ZMW experiments subsequently resumed accommodating tRNAs (Figure 3F). These severely malfunctioning ribosomes can also become candidates for termination by release factors in vivo (Dunkle and Cate, 2010), aborting translation after significant energy expenditure.

Paromomycin additionally prolongs the rotated state in general; however, this effect is weaker than apramycin. Paromomycin limits the classical/hybrid tRNA FRET fluctuations, favoring the classical state, which is not conducive for translocation, consistent with observations of Feldman et al. (2010). Alternatively, the stabilized, destacked conformation of A1492 and A1493 may conflict with EF-G function to reset the ribosome (Taylor et al., 2007). For both mechanisms, paromomycin effectively increases the energy barrier for the ribosome to translocate. Additionally, paromomycin can significantly lengthen the rotated lifetime of the first codon, but this is only observed at 10 μM paromomycin concentration. This suggests the presence of a secondary binding site; however, the mechanism for this codon-specific effect is not clear.

Gentamicin C, which also promotes the destacked A1492/A1493 conformation upon binding, induces miscoding as paromomycin. Gentamicin causes a similar increase in rotated ribosome lifetimes as well as locks the tRNAs into the classical conformation in tRNA-tRNA FRET experiments (Feldman et al., 2010). Additionally, gentamicin induces short-lived tRNA-binding events, like paromomycin in ZMW experiments. Unlike paromomycin, gentamicin increases the energy barrier to ribosome rotation across all codons, resulting in more severe disruptions than paromomycin. Gentamicin is 4,6 linked, and its ring III element contacts G1405 in the decoding site (Yoshizawa et al., 1998), whereas the additional ring contacts in 4,5 disubstituted aminoglycosides occur to the helical stem closed by C1409-G1491 (Fourmy et al., 1996). These different contacts and their effects on local and global ribosomal dynamics may explain the different mechanistic observations. Alternatively, secondary binding sites may also contribute. Intriguingly, gentamicin has the strongest inhibitory effect and is the most important of the three drugs in clinical applications.

Dissecting the Complex Effects of Aminoglycosides from Multiple Perspectives

By employing complementary single-molecule techniques, buttressed by structure and biochemical assays, our results provide a comprehensive understanding of aminoglycoside mechanisms. Their mode of action is far from simple and involves significant modifications to the delicate energy landscape of elongation. Aminoglycosides have distinct profiles of elongation inhibition, and their structural diversity indeed translates into a diversity of mechanisms. While aminoglycosides are thought to be effective by inducing miscoding and hindering

translocation, we have observed significant differences in the level of miscoding and effects on steps not directly linked to translocation, which for paromomycin and gentamicin were stronger than their effects on translocation. Despite the complexity of their mechanism, a common theme emerges where they significantly increase energy barriers for the ribosome subunits to rotate and to translocate. As the 1.5- to 4-fold inhibitions over each codon to various steps of the elongation cycle accumulate across multiple codons, these drugs can effectively stall the ribosome and cause severe disruptions to elongation. In fact, even with our 12-codon model mRNA, we already see a dramatic decrease in the number of codons translated during our observation timeframe. These observations agree with the original discussions of Kurland (Kurland, 1987) and others that aminoglycosides are bacteriocidal because of their inhibition of elongation efficiency, not miscoding. How the local conformational changes caused by aminoglycoside binding to the 30S decoding site affect the global behavior of the ribosome and how miscoding aminoglycosides modify the balance of tRNA selection fidelity versus efficiency remain open questions (Johansson et al., 2012).

EXPERIMENTAL PROCEDURES

Single-Molecule Reagents and Buffers

Fluorescently labeled 30S (Cy3 or Cy3B) and 50S (Cy5) subunits, wild-type 30S and 50S subunits, translation factors, S1, mRNA, fluorescently labeled tRNA (fMet-[Cy3]tRNA^{fMet}, Phe-[Cy5]tRNA^{Phe}, and Lys-[Cy2]tRNA^{Lys}), and unlabeled tRNA (fMet-tRNA^{fMet}, Phe-tRNA^{Phe}, and Lys-tRNA^{Lys}) were prepared as previously described (Blanchard et al., 2004b; Dorywalska et al., 2005; Marshall et al., 2008). All experiments were conducted in a Tris-based polymix buffer consisting of 50 mM Tris-acetate (pH 7.5), 100 mM potassium chloride, 5 mM ammonium acetate, 0.5 mM calcium acetate, 5 mM magnesium acetate, 0.5 mM EDTA, 5 mM putrescine-HCl, and 1 mM spermidine. All experiments also contained 4 mM GTP. The aminoglycosides used in this study were purchased from Sigma as dry powders and dissolved in water to make stock solutions.

The 5′ biotinylated mRNAs for the intersubunit FRET and ZMW experiments contained the 5′ UTR and Shine-Dalgarno sequence of T4 *gene 32* followed by either three Phe (UUU) codons (3F) or six alternating Phe (UUC) and Lys (AAA) codons (6(FK)). Both 6(FK) and 3F have a stop codon after the end of the message followed by an additional 4 Phe (UUU) codons (Aitken and Puglisi, 2010). The mRNAs for tRNA-tRNA FRET experiments either contain the full T4 *gene 32* sequence up to the 7th translated codon (MFK) or have the second translated codon changed from Phe (UUU) to a Leu (CUU) (MLK). All mRNAs were chemically synthesized by Dharmacon.

NMR Solution Structure of Apramycin in Complex with A-Site Oligonucleotide Mimic

Near-complete assignment of the proton resonances from the apramycin-RNA complex was accomplished using standard multidimensional, homonuclear, and heteronuclear experiments with unlabeled RNA, and uniformly ^{13}C, ^{15}N-labeled RNA samples (Lukavsky et al., 2003; Lukavsky and Puglisi, 2005). A total of 612 nuclear Overhauser effect (NOE) distance restrains were determined from two-dimensional (2D) and three-dimensional (3D) NOE spectroscopy (NOESY) experiments, of which 32 were intermolecular RNA-apramycin distance restraints. Distance restraints were categorized based on peak intensity into four groups with the following interproton distances: strong (1.8–3.5 Å), medium (2.0–4.5 Å), weak (2.2–6.0 Å), and very weak (3.0–7.0 Å). Dihedral restrains, β, ε, χ, were determined from 3D HCP, 3D heteronuclear multiple quantum coherence (HMQC) total correlation spectroscopy (TOCSY), and 2D NOESY experiments, respectively. Residual dipolar coupling restraints from aromatic N–H and C–H bond vectors were determined by comparing J-coupling constants collected from 2D 13C/15N transverse relaxation optimized spectroscopy (TROSY) spectra in the presence and absence of pf1 bacteriophage. Residual dipolar couplings (RDCs) were determined according to the following formula:

$$^{1}D_{XH} = {}^{1}J_{XH}(\text{with phage}) - {}^{1}J_{XH}(\text{without phage}),$$

where $^{1}D_{XH}$ is the dipolar coupling and $^{1}J_{XH}$ is the one bond scalar coupling for X = ^{13}C or ^{15}N. The magnitude of C–H RDCs were normalized to those collected for N–H bonds. A breakdown of the restraints used to determine the structure of the apramycin-RNA complex is shown in Table S2. Structures were calculated according to a previously published multistep simulated annealing protocol using only distance and dihedral restraints during the first stage implemented in XPLOR (Wimberly et al., 1993). RDCs were incorporated into the structure determination during a second stage, as described previously in CNS (Lynch et al., 2003).

Intersubunit FRET Experiments

We mixed 0.25 μM Cy3B-30S, preincubated with stoichiometric S1, 1 μM IF2, 1 μM fMet-tRNA^{fMet}, 1 μM 5′ biotinylated mRNA, and 4 mM GTP to form 30S preinitiation complexes (PICs) in the Tris-based polymix buffer described above to form 30S PICs (Dorywalska et al., 2005). The PIC mixture was incubated at 37°C for 5 min.

Before immobilizing the 30S PICs on a slide surface, we diluted the mixture with the Tris-based polymix buffer with 1 μM IF2 and 4 mM GTP. The PICs were then immobilized on the surface of a biotin-polyethylene glycol (PEG)-derivatized quartz slide via biotin-neutravidin interactions. We then washed excessive unbound material with the Tris-based polymix buffer containing 1 μM IF2, 4 mM GTP, 1 mM Trolox (to stabilize Cy5 photophysics), and an oxygen-scavenging system (2.5 mM 3,4-dihydroxybenzoic acid and 250 nM protocatechuate deoxygenase; Aitken et al., 2008). We delivered 50 nM Cy5-50S, 1 μM IF2, 80 or 160 nM EF-G, 80 nM ternary complexes, and aminoglycosides (where applicable at the indicated concentration) in the Tris-based polymix buffer using a controlled syringe pump to initiate translation. Phe-tRNA^{Phe} and Lys-tRNA^{Lys} ternary complexes with EF-Tu(GTP) were formed immediately before delivery, as previously described (Marshall et al., 2008).

ZMW Experiments

The preparation for ZMW experiments was the same as intersubunit experiments with the following exceptions. The first incubation mixture contains 0.25 μM unlabeled wild-type 30S, 0.25 μM wild-type 50S, 1 μM fMet-(Cy3) tRNAfMet, 1 μM 5′ biotinylated mRNA, and 4 mM GTP to form 70S initiation complexes (ICs). The 70S ICs are then immobilized using the same procedure as in intersubunit FRET experiments. The delivery mixture contained 1 μM IF2, 200 nM EF-G, 200 nM Phe-(Cy5)tRNA^{Phe} ternary complexes, 200 nM Lys-(Cy2)tRNA^{Lys} ternary complexes, and 10 μM paromomycin, apramycin, or gentamicin, comparable to intersubunit FRET conditions.

tRNA-tRNA FRET Experiments

The preparation for tRNA-tRNA FRET experiments was the same as ZMW experiments with the following exception. The delivery mixture contains 1 μM IF2, 500 nM EF-G (where applicable), 25 nM Phe-(Cy5)tRNA^{Phe} ternary complexes, and 10 μM aminoglycosides (where applicable).

Bulk Kinetic Experiments

Bulk kinetic experiments were performed at 20°C and pH 7.5 in polymix buffer (95 mM KCl, 5 mM NH_4Cl, 5 mM $Mg(OAc)_2$, 0.5 mM $CaCl_2$, 8 mM putrescine, 1 mM spermidine, 5 mM potassium phosphate, and 1 mM DTE) complemented with an energy supply and regeneration system consisting of 2 mM (ATP + GTP), 10 mM phosphoenolpyruvate, pyruvate kinase, and myokinase (Johansson et al., 2011). In the experiments for simultaneous monitoring of dipeptide formation and GTP hydrolysis, preinitiated 70S ribosomal complexes, carrying f[^{3}H]Met-tRNA^{fMet} in P site and displaying the Phe codon UUC in A site, were rapidly mixed with preformed Phe-tRNA^{Phe}:EF-Tu:[^{3}H]GTP ternary complex in a quench-flow instrument (RQF-3, KinTek Corp.) to a final concentration of 200 nM. The reactions were quenched with formic

acid at different incubation times and the fractions of products, [^{3}H]GDP/([^{3}H]GDP + [^{3}H]GTP) and f[^{3}H]Met-Phe/(f[^{3}H]Met-Phe + f[^{3}H]Met), were estimated by high-performance liquid chromatography (HPLC) as described (Johansson et al., 2011). The rates of GTP hydrolysis and dipeptide formation were measured in the presence (10 μM) and absence of each drug. The rate of GTP hydrolysis, k_{GTP}, including the association of ternary complex to the ribosome, and the rate of tRNA accommodation/peptidyl transfer, k_{pep}, obtained from the inverse of the difference between the dipeptide formation time and GTP hydrolysis time (Johansson et al., 2011) were estimated in drug absence and in the presence of each one of the drugs. Tripeptide formation was performed by rapid mixing and quenching of mixtures similar to those used for dipeptide bond formation, but with EF-G and EF-Ts added to the ternary complex mix and use of unlabeled rather than labeled GTP.

For further details, please refer to Extended Experimental Procedures.

SUPPLEMENTAL INFORMATION

Supplemental Information includes Extended Results, Extended Discussion, Extended Experimental Procedures, six figures, and two tables and can be found with this article online at http://dx.doi.org/10.1016/j.celrep.2013.01.027.

LICENSING INFORMATION

ACKNOWLEDGMENTS

Supported by NIH grant GM51266 (to J.D.P.), the Japan Science and Technology Agency (to S.U.), the Swedish Research Council (to M.E.), and the Knut and Alice Wallenberg Foundation (to M.E.). We thank Alexey Petrov (Stanford), Jin Chen (Stanford), and Seán O'Leary (Stanford) for valuable discussions. J.K. is an employee and stock option holder, and J.D.P. is a consultant of Pacific Biosciences, a company commercializing sequencing technologies.

Received: August 5, 2012
Revised: November 18, 2012
Accepted: January 22, 2013
Published: February 14, 2013

REFERENCES

Aitken, C.E., and Puglisi, J.D. (2010). Following the intersubunit conformation of the ribosome during translation in real time. Nat. Struct. Mol. Biol. *17*, 793–800.

Aitken, C.E., Marshall, R.A., and Puglisi, J.D. (2008). An oxygen scavenging system for improvement of dye stability in single-molecule fluorescence experiments. Biophys. J. *94*, 1826–1835.

Aitken, C.E., Petrov, A., and Puglisi, J.D. (2010). Single ribosome dynamics and the mechanism of translation. Annu. Rev. Biophys. *39*, 491–513.

Benveniste, R., and Davies, J. (1973). Structure-activity relationships among the aminoglycoside antibiotics: role of hydroxyl and amino groups. Antimicrob. Agents Chemother. *4*, 402–409.

Blanchard, S.C., Gonzalez, R.L., Kim, H.D., Chu, S., and Puglisi, J.D. (2004a). tRNA selection and kinetic proofreading in translation. Nat. Struct. Mol. Biol. *11*, 1008–1014.

Blanchard, S.C., Kim, H.D., Gonzalez, R.L., Jr., Puglisi, J.D., and Chu, S. (2004b). tRNA dynamics on the ribosome during translation. Proc. Natl. Acad. Sci. USA *101*, 12893–12898.

Borovinskaya, M.A., Pai, R.D., Zhang, W., Schuwirth, B.S., Holton, J.M., Hirokawa, G., Kaji, H., Kaji, A., and Cate, J.H. (2007). Structural basis for aminoglycoside inhibition of bacterial ribosome recycling. Nat. Struct. Mol. Biol. *14*, 727–732.

Böttger, E.C. (2006). The ribosome as a drug target. Trends Biotechnol. *24*, 145–147.

Böttger, E.C., Springer, B., Prammananan, T., Kidan, Y., and Sander, P. (2001). Structural basis for selectivity and toxicity of ribosomal antibiotics. EMBO Rep. *2*, 318–323.

Brodersen, D.E., Clemons, W.M., Jr., Carter, A.P., Morgan-Warren, R.J., Wimberly, B.T., and Ramakrishnan, V. (2000). The structural basis for the action of the antibiotics tetracycline, pactamycin, and hygromycin B on the 30S ribosomal subunit. Cell *103*, 1143–1154.

Cabañas, M.J., Vázquez, D., and Modolell, J. (1978). Dual interference of hygromycin B with ribosomal translocation and with aminoacyl-tRNA recognition. Eur. J. Biochem. *87*, 21–27.

Carter, A.P., Clemons, W.M., Brodersen, D.E., Morgan-Warren, R.J., Wimberly, B.T., and Ramakrishnan, V. (2000). Functional insights from the structure of the 30S ribosomal subunit and its interactions with antibiotics. Nature *407*, 340–348.

Davies, J., and Davis, B.D. (1968). Misreading of ribonucleic acid code words induced by aminoglycoside antibiotics. The effect of drug concentration. J. Biol. Chem. *243*, 3312–3316.

Davies, J., Gorini, L., and Davis, B.D. (1965). Misreading of RNA codewords induced by aminoglycoside antibiotics. Mol. Pharmacol. *1*, 93–106.

Dorywalska, M., Blanchard, S.C., Gonzalez, R.L., Kim, H.D., Chu, S., and Puglisi, J.D. (2005). Site-specific labeling of the ribosome for single-molecule spectroscopy. Nucleic Acids Res. *33*, 182–189.

Dunkle, J.A., and Cate, J.H. (2010). Ribosome structure and dynamics during translocation and termination. Annu. Rev. Biophys. *39*, 227–244.

Feldman, M.B., Terry, D.S., Altman, R.B., and Blanchard, S.C. (2010). Aminoglycoside activity observed on single pre-translocation ribosome complexes. Nat. Chem. Biol. *6*, 54–62.

Fourmy, D., Recht, M.I., Blanchard, S.C., and Puglisi, J.D. (1996). Structure of the A site of Escherichia coli 16S ribosomal RNA complexed with an aminoglycoside antibiotic. Science *274*, 1367–1371.

Fourmy, D., Yoshizawa, S., and Puglisi, J.D. (1998). Paromomycin binding induces a local conformational change in the A-site of 16 S rRNA. J. Mol. Biol. *277*, 333–345.

François, B., Russell, R.J., Murray, J.B., Aboul-ela, F., Masquida, B., Vicens, Q., and Westhof, E. (2005). Crystal structures of complexes between aminoglycosides and decoding A site oligonucleotides: role of the number of rings and positive charges in the specific binding leading to miscoding. Nucleic Acids Res. *33*, 5677–5690.

Green, R., and Noller, H.F. (1997). Ribosomes and translation. Annu. Rev. Biochem. *66*, 679–716.

Johansson, M., Ieong, K.W., Trobro, S., Strazewski, P., Åqvist, J., Pavlov, M.Y., and Ehrenberg, M. (2011). pH-sensitivity of the ribosomal peptidyl transfer reaction dependent on the identity of the A-site aminoacyl-tRNA. Proc. Natl. Acad. Sci. USA *108*, 79–84.

Johansson, M., Zhang, J., and Ehrenberg, M. (2012). Genetic code translation displays a linear trade-off between efficiency and accuracy of tRNA selection. Proc. Natl. Acad. Sci. USA *109*, 131–136.

Korostelev, A., Ermolenko, D.N., and Noller, H.F. (2008). Structural dynamics of the ribosome. Curr. Opin. Chem. Biol. *12*, 674–683.

Kurland, C.G. (1987). The error catastrophe: a molecular Fata Morgana. BioEssays *6*, 33–35.

Lee, T.H., Blanchard, S.C., Kim, H.D., Puglisi, J.D., and Chu, S. (2007). The role of fluctuations in tRNA selection by the ribosome. Proc. Natl. Acad. Sci. USA *104*, 13661–13665.

Levene, M.J., Korlach, J., Turner, S.W., Foquet, M., Craighead, H.G., and Webb, W.W. (2003). Zero-mode waveguides for single-molecule analysis at high concentrations. Science *299*, 682–686.

Lukavsky, P.J., and Puglisi, J.D. (2005). Structure determination of large biological RNAs. Methods Enzymol. *394*, 399–416.

Lukavsky, P.J., Kim, I., Otto, G.A., and Puglisi, J.D. (2003). Structure of HCV IRES domain II determined by NMR. Nat. Struct. Biol. *10*, 1033–1038.

Lynch, S.R., Gonzalez, R.L., and Puglisi, J.D. (2003). Comparison of X-ray crystal structure of the 30S subunit-antibiotic complex with NMR structure of decoding site oligonucleotide-paromomycin complex. Structure *11*, 43–53.

Marshall, R.A., Dorywalska, M., and Puglisi, J.D. (2008). Irreversible chemical steps control intersubunit dynamics during translation. Proc. Natl. Acad. Sci. USA *105*, 15364–15369.

Matt, T., Ng, C.L., Lang, K., Sha, S.H., Akbergenov, R., Shcherbakov, D., Meyer, M., Duscha, S., Xie, J., Dubbaka, S.R., et al. (2012). Dissociation of antibacterial activity and aminoglycoside ototoxicity in the 4-monosubstituted 2-deoxystreptamine apramycin. Proc. Natl. Acad. Sci. USA *109*, 10984–10989.

Moazed, D., and Noller, H.F. (1990). Binding of tRNA to the ribosomal A and P sites protects two distinct sets of nucleotides in 16 S rRNA. J. Mol. Biol. *211*, 135–145.

Nilsson, J., and Nissen, P. (2005). Elongation factors on the ribosome. Curr. Opin. Struct. Biol. *15*, 349–354.

Ogle, J.M., Brodersen, D.E., Clemons, W.M., Jr., Tarry, M.J., Carter, A.P., and Ramakrishnan, V. (2001). Recognition of cognate transfer RNA by the 30S ribosomal subunit. Science *292*, 897–902.

Pape, T., Wintermeyer, W., and Rodnina, M.V. (1998). Complete kinetic mechanism of elongation factor Tu-dependent binding of aminoacyl-tRNA to the A site of the E. coli ribosome. EMBO J. *17*, 7490–7497.

Pape, T., Wintermeyer, W., and Rodnina, M.V. (2000). Conformational switch in the decoding region of 16S rRNA during aminoacyl-tRNA selection on the ribosome. Nat. Struct. Biol. *7*, 104–107.

Perzynski, S., Cannon, M., Cundliffe, E., Chahwala, S.B., and Davies, J. (1979). Effects of apramycin, a novel aminoglycoside antibiotic on bacterial protein synthesis. Eur. J. Biochem. *99*, 623–628.

Powers, T., and Noller, H.F. (1991). A functional pseudoknot in 16S ribosomal RNA. EMBO J. *10*, 2203–2214.

Recht, M.I., Fourmy, D., Blanchard, S.C., Dahlquist, K.D., and Puglisi, J.D. (1996). RNA sequence determinants for aminoglycoside binding to an A-site rRNA model oligonucleotide. J. Mol. Biol. *262*, 421–436.

Recht, M.I., Douthwaite, S., and Puglisi, J.D. (1999). Basis for prokaryotic specificity of action of aminoglycoside antibiotics. EMBO J. *18*, 3133–3138.

Selmer, M., Dunham, C.M., Murphy, F.V., 4th, Weixlbaumer, A., Petry, S., Kelley, A.C., Weir, J.R., and Ramakrishnan, V. (2006). Structure of the 70S ribosome complexed with mRNA and tRNA. Science *313*, 1935–1942.

Taylor, D.J., Nilsson, J., Merrill, A.R., Andersen, G.R., Nissen, P., and Frank, J. (2007). Structures of modified eEF2 80S ribosome complexes reveal the role of GTP hydrolysis in translocation. EMBO J. *26*, 2421–2431.

Tsai, A., Petrov, A., Marshall, R.A., Korlach, J., Uemura, S., and Puglisi, J.D. (2012). Heterogeneous pathways and timing of factor departure during translation initiation. Nature *487*, 390–393.

Uemura, S., Aitken, C.E., Korlach, J., Flusberg, B.A., Turner, S.W., and Puglisi, J.D. (2010). Real-time tRNA transit on single translating ribosomes at codon resolution. Nature *464*, 1012–1017.

Wimberly, B., Varani, G., and Tinoco, I., Jr. (1993). The conformation of loop E of eukaryotic 5S ribosomal RNA. Biochemistry *32*, 1078–1087.

Wintermeyer, W., Peske, F., Beringer, M., Gromadski, K.B., Savelsbergh, A., and Rodnina, M.V. (2004). Mechanisms of elongation on the ribosome: dynamics of a macromolecular machine. Biochem. Soc. Trans. *32*, 733–737.

Woodcock, J., Moazed, D., Cannon, M., Davies, J., and Noller, H.F. (1991). Interaction of antibiotics with A- and P-site-specific bases in 16S ribosomal RNA. EMBO J. *10*, 3099–3103.

Yonath, A. (2005). Antibiotics targeting ribosomes: resistance, selectivity, synergism and cellular regulation. Annu. Rev. Biochem. *74*, 649–679.

Yoshizawa, S., Fourmy, D., and Puglisi, J.D. (1998). Structural origins of gentamicin antibiotic action. EMBO J. *17*, 6437–6448.

Yoshizawa, S., Fourmy, D., and Puglisi, J.D. (1999). Recognition of the codon-anticodon helix by ribosomal RNA. Science *285*, 1722–1725.

Zaher, H.S., and Green, R. (2009). Fidelity at the molecular level: lessons from protein synthesis. Cell *136*, 746–762.